Spatial Modeling Of Red Spider Mite *Oligonychus Punicae* (Acari: Tetranychidae) In Avocado Crop

Isidro Audberto Campos-Tarango[1], José Francisco Ramírez-Dávila[3,*], Dulce Karen Figueroa-Figueroa[2], Fidel Lara-Vázquez[2], Andres Gonzalez-Huerta[2].

[1]Autonomous University of the State of Mexico, Cerrillo Piedras Blancas n/n km 15, Toluca, 50200, Mexico.

[2]Teacher of [1]Autonomous University of the State of Mexico, Cerrillo Piedras Blancas n/n km 15, Toluca, 50200, Mexico.

[3]Laboratory of Entomology Research and Technology in Precision Farming, UAEM, Cerrillo Piedras Blancas n/n km 15, Toluca, 50200, México.

*Corresponding Author: José Francisco Ramírez-Dávila. Email: jframirezd@uaemex.mx.

Abstract: In recent years, there has been a rising concern in society to produce quality food in a sustainable manner that is the reason new alternatives in pest control have been researched so they help mitigate the environmental impact. In traditional agriculture, pesticides are applied uniformly, without considering spatial and temporary variables, doses can be focused according to the incidence with the help of maps; thus contributing to improve environmental balance and production costs. Among these crops, avocado (*Persea americana*) generates huge economic benefits in the localities where this crop exists. Among the main pests that attack this crop is found red spider mite (*Oligonychus punicae*), which causes damage to the epidermis of the leaves in such a way that the injured areas discolor and the edges of the leaves are deformed as a result of the removal of the cellular content from the tissues. Therefore the objective of the present work was the determination of the spatial pattern this pest has, by means of Geostatistics and SADIE indices. The results show that red spider mite is distributed in aggregation clusters and conform to Gaussian and Spherical models. Also, the infested surface was determined through maps, with which control programs can be carried out directing control measures to the areas with the highest incidence.

Key words: MITES, geostatistics, kriging, density maps, saide.

Introduction

Avocado (*Persea americana* Mill) Cv. Hass is one of the main fruit crops in Mexico because its importance in national and international markets. Its worldwide production is estimated in 4,2 millions of tons, Mexico is the most important producer with an annual average production of 1,8 millions of tons distributed in 205 thousand ha, with a yield of 10,18 ton/ha [1].

Avocado crop presents a large number of pests, among them: thrips (*Frankliniella* spp.), mites (*Oligonychus punicae* Hirst. y *O. perseae* Tuttle), trunk and branch borer (*Copturus aguacatae* Kissinger), avocado leafhopper (*Idona minuenda* Ball), whiteflies (*Tetraleurodes* spp.), avocado leafroller (*Amorbia cunneana* Walsingham) and avocado leafminer (*Gracilaria perseae* Busck), seed borer (*Conotrachelus perseae* Barber y *C. aguacatae* Barber) [2].

Among the aforementioned pests the mite *Oligonychus punicae* (Hirst) (Acari: Tetranychidae), also known as red spider mite, has become really important to avocado crop because it feeds on the foliage, by inserting its stilettos into the plant tissue, causing reddish spots. When damage is severe, it causes the collapse of mesophyll, which results in the defoliation and loss of production. It is present all year around, but it has its higher incidence in spring and autumn. Traditionally, to control this pest chemical products were utilized; however they have lost their efficacy due to resistance, provoking residuality problems. This pest is distributed in North and South America, as well as in European and Asian countries [3, 4].

Monitoring of populations of *O. punicae* is necessary to know how this mite populations are distributed in the plots, knowing the actual impact they have in avocado crop, would help to elaborate control strategies. Therefore the objective of the present work was to determine the spatial distribution of *O. punicae* in avocado crop by usage of geostatistical techniques.

Materials and methods

The study was carried out in the municipalities of Tenancingo de Degollado (18°57′ N y 99°35′ W) average altitude 2031 masl and Temascaltepec (19°02′ N y 100°02′ N) average altitude 1,740 masl, in eight two-ha plots per municipality. They were subject to the same agronomic management without application of pesticides. Sampling was done by quadrant methodology, which consists of dividing the plot in 50 quadrants of 20 x 20 m 25 quadrants were randomly taken per plot where two trees were selected, each one of the 50 trees per plot was marked and georeferenced using a GPSmap60 (Garmin) to obtain its coordinates. A monthly sampling was carried out from October 2019 to May 2020. The number of mites per leaf was counted with a magnification lens 20X 60 leaves per tree were selected taking fifteen divided in three strata (lower, middle and upper), in each cardinal point of the tree (North, East, West and South) [5, 6, 7, 8, 9].

Geostatistical Analysis

The experimental semivariogram was estimated with data obtained from different samples of populations of *O. punicae* [11]. The value of the experimental semivariogram was calculated with the following formula.

$$r^*(h) = \frac{1}{2N(h)} \sum_{i=1}^{N(H)} [z(x_i + h) - z(x_i)]^2 \qquad (1)$$

Where: γ*(h) is the experimental value of the semivariogram for lag h; N(h) is the number of pairs of points separated by h; z(xi) is the value of the variable of interest in the sample point xi; z(xi+h) is the value of the variable of interest in the sample point xi+h. Obtaining the experimental semivariograms was done with the software Variowin 2,2 (Software Forspatial Data Analysis in 2D. Springer Verlag, New York USA) [6, 7, 8, 12].

The experimental semivariogram obtained was adjusted to a theoretical semivariogram. Theoretical models commonly used to adjust experimental semivariograms are: spherical, exponential, Gaussian, logarithmic, pure nugget effect, hole effect and monomic. Once the experimental semivariogram was obtained, it was adjusted to the theoretical semivariogram. At last nugget effect, sill and range values were determined [9, 10, 13, 14]. Validation of theoretical model was carried out interactively, varying the values ‘Co’ (nugget effect), ‘C + Co’ (sill) and ‘a’ (range), until the best fit

was obtained. Once determined was validated through the determination of statistical parameters of cross validation as: mean of estimation errors (MEE), mean quadratic error (ECM) and mean dimensionless quadratic error (ECMA) [15, 16] these statistics are as follows:

a) Mean of estimation errors (MEE):

$$MEE = \frac{1}{n}\sum_{i=1}^{n}[z^*(x_i) - z(x_i)] \qquad (2)$$

Where: z*(xi) is the estimated value of the variable of interest in the point xi; z(xi) is the measured value of the variable of interest in the point xi and n is the number of sample points used in the interpolation. MEE should not be significantly different from 0 (t test), which indicates that the semivariogram model allows the calculation of unbiased estimators.

b) Mean quadratic error (ECM):

$$ECM = \frac{1}{n}\sum_{i=1}^{n}[z^*(x_i) - z(x_i)]^2 \qquad (3)$$

A semivariogram model is considered adequate if, as a rule of thumb, the value of the statistic is close to cero.

c) Mean dimensionless quadratic error (ECMA):

$$ECMA = \frac{1}{n}\sum_{i=1}^{n}\frac{[z^*(x_i) - z(x_i)]}{\sigma k} \qquad (4)$$

Where: σk is the standard deviation of the expected error in the estimation with the kriging. The validity of the model is satisfied if ECMA is between the values $1\pm2\ (2/N)^{0.5}$.

d) Another statistic to validate the model consists in the variance value of the errors being less than the sample variance.

The level of spatial dependence was calculated in order to determine the degree of relationship that the corresponding data store. This value is obtained by dividing the nugget effect by the sill, and the result is expressed in percentage, less than 25% is high, between 26% and 75% is moderated and over 76% is low [9, 10, 18].

Finally, density maps were produced, once the semivariogram models were validated, the spatial interpolation was performed using the kriging method, which allows the unbiased estimation of values associated to points that were not sampled; to elaborate the maps the program Surfer 9 (Surface Mapping System, Golden Software Inc. 809, 14th Street. Golden, Colorado 80401-1866. USA) was

used. The estimation of the infested surface was carried out with the density maps for each sampled date [6, 7, 8, 19]

SADIE (Spatial Analysis by Distance Indices).

The theoretical basis of this kind of analysis consists in the evaluation of objects or entities, on the basis of knowledge of its situation in space, being a methodology of spatial statistics, which identifies a spatial model for bidimensional data, has an index associated to aggregation and a test for deviation of randomness based in an attraction algorithm, which incorporates a biological model for the dispersion of individuals of an origin in which each individual is assigned a dynamic territory. It is a biological index more descriptive and informative of the insect population spatial distribution than the dispersion index (average ratio variance) and the Green Index, which depend directly on the abundance of the population [20, 40]. [39] indicated that for data collected at specific locations, the usage of distance to regularity is very appropriate and demonstrated how to distinguish non randomness in the form of statistical heterogeneity, from the spatial non randomness he developed and extended the usage of distance index of aggregation (*Ia*) to establish de spatial structure of the insect populations and the index to estimate the number of clusters of a population (*Ja*).

Therefore, the sample is aggregated if $Ia > 1$, it is random if $Ia = 1$ and it is regular if $Ia < 1$; on the other hand, if $Ja > 1$ it is aggregated, if $Ja = 1$ data is spatially random and if $Ja < 1$ the sample is regular. The values of *Ja* index are used to confirm the results obtained with the *Ia* index. To determine the significance with respect to the unit its respective probability is used (*Oa*) [21]. The program used was SADIE 1,22 [20].

Results

The spatial behavior that different avocado attacking pests is closely related to environmental factors, such as habitat distribution, microclimate and food availability. With the results of the monthly sampling it was possible to carry out the modeling and mapping of the populations of *O. punicae* in the avocado plots. It was reached to determine the spatial behavior of this mite in the short term, establishing the percentage of infestation in each sampling per plot.

The average of the populations of *O. punicae* varied within plots and date of sampling; for Tenancingo municipality the lowest density was registered in December in plot one with 21,62; for Temascaltepec municipality the lowest density was registered in plot five in November with 41,02. The highest densities were registered in May with 288,64 and 328,58 in plots four and five in the municipalities of Tenancingo and Temascaltepec, respectively (Table 1).

The spatial distribution in commercial avocado plots presented by *O. p nicae u*is aggregated in each one of the sampled dates. The experimental semivariograms obtained in the plots at Tenancingo municipality best fitted the Spherical (17) and Gaussian (15) models; in plot one in November and May they fitted the Gaussian model, the rest of the months they fitted the Spherical model. In the municipality of Temascaltepec, experimental semivariograms fitted Spherical (22) and Gaussian (10) models, in plot eight, October, April and May dataset fitted Gaussian model, the rest of the months fitted Spherical model (Table 1). For all fitted models nugget effect was cero, so the sampling error was considered minimal and the sampling scale for each locality was appropriate.

Table 1. Parameters of the theoretical models fitted to the semivariograms of *O. punicae*, in the Tenancingo Municipality (Plots 1, 2, 3 and 4) and Temascaltepec Municipality (Plots 5, 6, 7 and 8).

P.	Date	Model	Mean Density	Min.	Max.	Nugget	Hill	Range	Nugget/ Hill	Spatial dependence level	%
1	October 2019	Spherical	32,90	1	69	0	302,46	25,70	0	High	92
	November 2019	Gaussian	24,72	0	62	0	270,00	26,64	0	High	90
	December 2019	Spherical	21,62	0	55	0	228,15	39,10	0	High	88
	January 2020	Spherical	24,14	4	59	0	176,00	22,00	0	High	91
	February 2020	Spherical	52,58	27	94	0	285,80	32,56	0	High	86
	March 2020	Spherical	64,52	38	113	0	324,17	29,60	0	High	84
	Aprill 2020	Spherical	98,18	47	180	0	662,20	32,56	0	High	85
	May 2020	Gaussian	283,76	148	528	0	2571,40	22,95	0	High	95
2	October 2019	Spherical	31,38	1	65	0	319,43	12,79	0	High	89
	November 2019	Spherical	31,32	0	68	0	392,59	31,91	0	High	91
	December 2019	Gaussian	38,88	4	82	0	497,28	15,59	0	High	94
	January 2020	Spherical	39,68	4	83	0	622,50	29,40	0	High	90
	February 2020	Gaussian	49,7	5	104	0	960,00	31,17	0	High	92
	March 2020	Gaussian	79,44	15	133	0	1344,76	24,00	0	High	97
	April 2020	Gaussian	132,70	63	193	0	845,32	31,73	0	High	98
	May 2020	Spherical	287,00	132	490	0	2630,61	26,60	0	High	95
3	October 2019	Gaussian	28,94	1	59	0	273,98	20,61	0	High	88
	November 2019	Gaussian	29,04	2	60	0	285,60	28,88	0	High	87
	December 2019	Spherical	33,32	5	62	0	289,57	49,70	0	High	90
	January 2020	Spherical	34,00	4	68	0	348,30	34,00	0	High	91
	February 2020	Gaussian	41,66	7	79	0	508,40	26,60	0	High	86
	March 2020	Spherical	72,52	20	117	0	65373	33,44	0	High	93
	April 2020	Gaussian	116,76	55	190	0	1130,59	26,67	0	High	90
	May 2020	Spherical	282,30	130	467	0	3333,33	28,94	0	High	96
4	October 2019	Spherical	32,12	1	62	0	270,00	17,88	0	High	87
	November 2019	Spherical	33,02	2	75	0	370,92	35,45	0	High	83
	December 2019	Gaussian	36,00	1	73	0	379,16	28,79	0	High	87
	January 2020	Gaussian	40,40	3	83	0	397,34	25,85	0	High	93
	February 2020	Gaussian	56,58	16	104	0	489,75	24,85	0	High	95
	March 2020	Spherical	65,50	21	113	0	570,00	35,25	0	High	94
	April 2020	Gaussian	104,68	52	172	0	861,26	30,75	0	High	89
	May 2020	Gaussian	288,64	175	520	0	2283,31	28,69	0	High	91
5	October 2019	Gaussian	43,94	13	63	0	256,00	26,62	0	High	92
	November 2019	Spherical	41,02	3	74	0	247,77	30,75	0	High	91
	December 2019	Spherical	44,56	12	82	0	230,33	30,00	0	High	88
	January 2020	Spherical	46,64	14	82	0	206,30	39,75	0	High	89
	February 2020	Gaussian	57,72	18	86	0	329,89	28,50	0	High	95
	March 2020	Spherical	67,66	17	97	0	405,00	45,00	0	High	96
	April 2020	Spherical	143,14	79	179	0	619,47	27,99	0	High	89
	May 2020	Gaussian	328,58	185	480	0	2628,37	24,08	0	High	94
6	October 2019	Spherical	48,98	17	82	0	344,64	27,59	0	High	84
	November 2019	Gaussian	45,14	9	87	0	367,50	25,50	0	High	87
	December 2019	Spherical	47,06	14	81	0	286,99	36,49	0	High	85
	January 2020	Spherical	54,04	17	83	0	272,89	33,00	0	High	86
	February 2020	Spherical	59,54	16	86	0	264,66	43,50	0	High	91
	March 2020	Spherical	76,14	37	97	0	200,82	40,50	0	High	93
	April 2020	Spherical	104,98	55	230	0	768,48	37,50	0	High	90
	May 2020	Spherical	292,28	80	539	0	3530,96	37,48	0	High	95
7	October 2019	Spherical	53,64	17	85	0	410,34	20,68	0	High	81
	November 2019	Gaussian	53,42	13	84	0	369,61	14,60	0	High	93
	December 2019	Gaussian	58,48	22	93	0	436,71	17,52	0	High	90
	January 2020	Spherical	61,80	23	97	0	429,49	13,90	0	High	78
	Febuary 2020	Gaussian	72,54	32	108	0	424,91	15,25	0	High	93
	March 2020	Spherical	84,06	48	118	0	386,07	21,17	0	High	90
	April 2020	Spherical	106,84	60	245	0	895,93	31,20	0	High	92
	May 2020	Spherical	292,86	140	461	0	3786,93	23,60	0	High	91
8	October 2019	Gaussian	50,19	7	74	0	453,70	14,56	0	High	88
	November 2019	Spherical	58,72	13	95	0	480,76	13,87	0	High	90
	December 2019	Spherical	60,94	18	100	0	430,08	18,25	0	High	92
	January 2020	Spherical	70,00	24	104	0	469,80	16,79	0	High	91

February 2020	Spherical	82,64	25	110	0	375,07	17,76	0	High	95
March 2020	Spherical	92,76	37	120	0	330,30	24,09	0	High	97
April 2020	Gaussian	127,20	76	225	0	959,07	23,90	0	High	86
May 2020	Gaussian	294,56	145	520	0	3383,73	19,23	0	High	92

P. = plot, Mín. = mínimum amount of mites per tree, Max. = máximum amount of mites per tree, S.D. = spatial dependence, %=infested surface.

The range indicates the maximum distance to which there is a spatial relation between the data; the range values that were presented on plot one belonging to Tenancingo were located between 22,00 m in January and 39,10 m in December, in this municipality the minimum range was 12,79 m and the maximum range was 49,70 m corresponding to plot two in October and plot three in December, respectively. For Temascaltepec municipality on plot six the range values fluctuated between 25,50 m and 43,5 m in November and February respectively, for total sampling in the municipality, the minimum range was 13,87 m on plot eight in November, and the maximum range was 45,00 m on plot five in March (Table 1).

The fitted models in each sample showed a high level of spatial dependence. The models that resulted from the spatial distribution of *O. punicae* were validated with the statistical parameters locating them within allowable range (Table 2).

Table 2. Values of Cross Validation Statistics of the Semivariograms of *Oligonychus punicae* Hirst, in the Municipality of Tenancingo (Plots 1, 2, 3, and 4) and municipality of Temascaltepec (Plots 5, 6, 7, and 8).

Plot	Date	Sampling variance	MEE*	Error variance	ECM	ECMA
1	October 2019	33,09	0,11	11,56	0,07	1,11
	November 2019	29,28	0,06	17,48	0,11	1,13
	December 2019	22,59	0,14	11,05	0,12	1,06
	January 2020	18,96	0,10	11,37	0,14	1,12
	February 2020	24,56	0,12	21,71	0,10	1,09
	March 2020	30,88	0,08	24,58	0,09	1,07
	April 2020	85,30	0,11	48,30	0,14	1,11
	May 2020	29,34	0,07	19,22	0,10	1,12
2	October 2019	34,63	0,13	16,41	0,12	1,14
	November 2019	40,81	0,12	31,52	0,07	1,11
	December 2019	58,98	0,09	39,85	0,09	1,10
	January 2020	67,81	0,13	43,87	0,11	1,09
	February 2020	83,05	0,10	61,25	0,13	1,10
	March 2020	11,60	0,08	10,28	0,10	1,14
	April 2020	88,65	0,11	79,59	0,08	1,12
	May 2020	26,94	0,14	18,77	0,12	1,11
3	October 2019	30,73	0,10	21,65	0,10	1,14
	November 2019	28,55	0,07	19,22	0,13	1,08
	December 2019	29,85	0,12	15,93	0,11	1,06
	January 2020	36,12	0,10	22,54	0,14	1,11
	February 2020	48,26	0,14	39,42	0,06	1,13
	March 2020	95,92	0,07	71,60	0,11	1,10
	April 2020	13,82	0,12	11,36	0,13	1,11
	May 2020	38,81	0,10	27,81	0,10	1,09
4	October 2019	35,26	0,09	21,66	0,12	1,12
	November 2019	40,45	0,13	32,25	0,08	1,07
	December 2019	39,28	0,11	24,71	0,13	1,14
	January 2020	43,24	0,09	29,53	0,10	1,12
	February 2020	48,64	0,10	36,92	0,07	1,10
	March 2020	65,57	0,13	51,31	0,11	1,13
	April 2020	98,81	0,10	78,46	0,13	1,11
	May 2020	27,27	0,08	18,76	0,10	1,10

Plot	Date	Sampling variance	MEE*	Error variance	ECM	ECMA
5	October 2019	26,21	0,10	11,31	0,13	1,12
	November 2019	31,77	0,08	21,44	0,09	1,14
	December 2019	24,00	0,12	17,29	0,10	1,07
	January 2020	19,83	0,14	11,36	0,14	1,10
	February 2020	30,00	0,09	23,82	0,06	1,11
	March 2020	39,34	0,13	21,75	0,10	1,13
	April 2020	75,88	0,11	51,43	0,13	1,07
	May 2020	28,28	0,07	16,29	0,10	1,10
6	October 2019	34,83	0,14	20,83	0,14	1,09
	November 2019	36,64	0,13	27,04	0,11	1,12
	December 2019	28,69	0,10	19,66	0,09	1,14
	January 2020	31,15	0,06	24,27	0,06	1,13
	February 2020	24,68	0,11	16,35	0,10	1,10
	March 2020	18,36	0,12	11,77	0,07	1,07
	April 2020	88,17	0,10	69,61	0,12	1,12
	May 2020	37,96	0,09	19,84	0,08	1,09
7	October 2019	42,47	0,13	31,51	0,13	1,13
	November 2019	40,12	0,10	29,62	0,11	1,11
	December 2019	43,16	0,14	30,56	0,14	1,08
	January 2020	38,48	0,07	23,29	0,10	1,14
	February 2020	36,80	0,13	21,38	0,12	1,06
	March 2020	34,37	0,12	28,25	0,07	1,10
	April 2020	99,29	0,08	71,38	0,11	1,07
	May 2020	39,92	0,11	20,74	0,06	1,11
8	October 2019	42,68	0,14	28,33	0,14	1,12
	November 2019	54,88	0,10	37,27	0,12	1,14
	December 2019	44,37	0,09	32,86	0,10	1,09
	January 2020	50,00	0,13	36,41	0,09	1,11
	February 2020	32,27	0,06	17,92	0,11	1,13
	March 2020	26,74	0,11	19,45	0,08	1,10
	April 2020	98,32	0,13	56,29	0,12	1,08
	May 2020	39,32	0,10	23,67	0,06	1,12

MEE = Estimation error mean, ECM = Mean quadratic error, ECMA = Dimensionless mean quadratic error.

Density mapping was carried out using the geostatistical method known as ordinary kriging once the corresponding semivariograms were validated. In these maps it is observed that *O. punicae* groups in aggregation clusters, being able to say that its distribution is located in specific aggregation clusters in different plot areas. This method was used because it allows to visualize its behavior in points not sampled with an unbiased estimate. In the case of plot one belonging to Tenancingo municipality surface maps for October, November and December show that aggregation clusters are distributed in the central part of the plot with a tendency towards the left side, in January, February and March, aggregation clusters were randomly distributed on the edges of the plot, while in April the infestation sites were located on the right side with a tendency towards the center; finally, in May there was only one significant aggregation cluster on the left side. It is noteworthy that in the last two months (April and May) the highest number of *O. punicae* is present due to the lack of rain in the study area favoring the population growth (Figure 1).

	Plot 1	Plot 2	Plot 3	Plot 4
October 2019	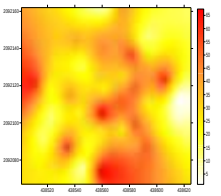	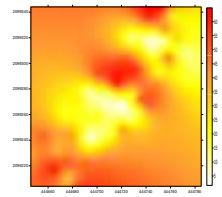	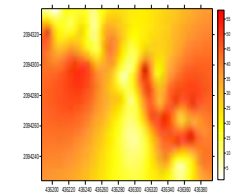	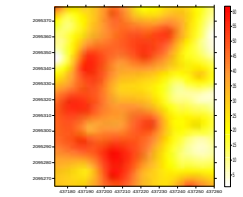
November 2019	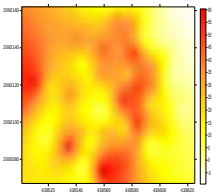	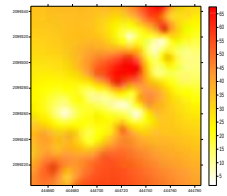	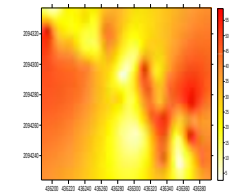	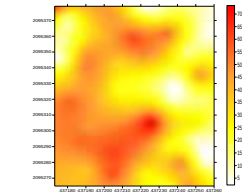
December 2019	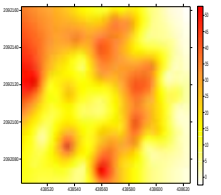	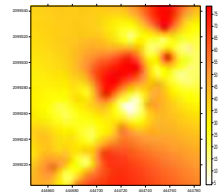	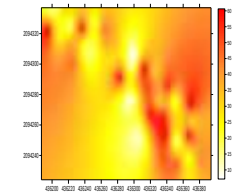	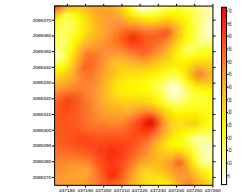
January 2020	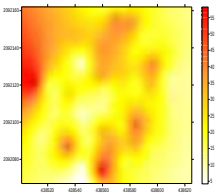	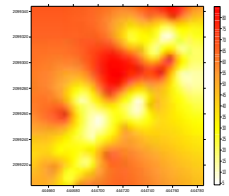	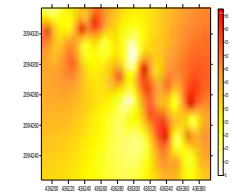	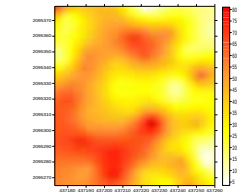
February 2020	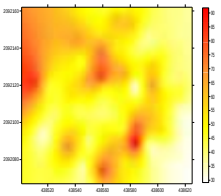	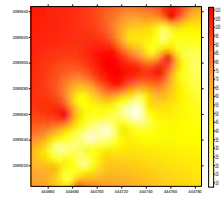	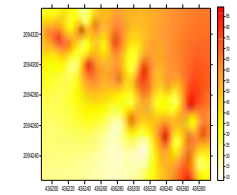	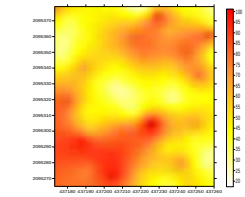
March 2020	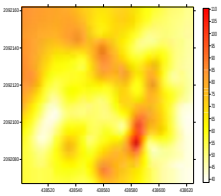	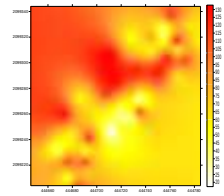	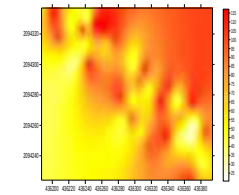	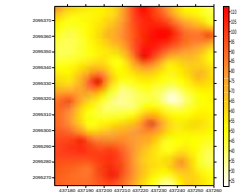
April 2020	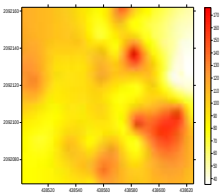	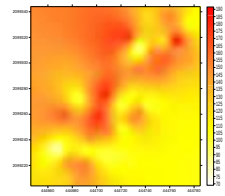	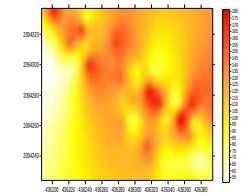	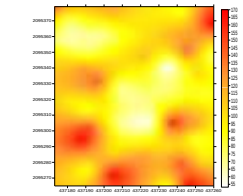

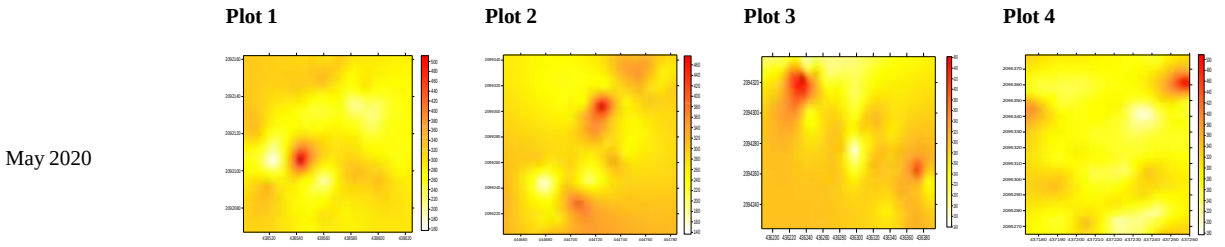

Figure 1. Density maps of *Oligonychus punicae* Hirst, in avocado crop, by sampling date in plots of Tenancingo municipality.

On plot five belonging to Temascaltepec municipality in October and November the infestation sites were located in the central part and on the left and right edges of the plot; with a downward trend on the left and towards the top on the right side, behavior is persistent with a minimal mobility, in December and January the infestation sites are concentrated in the central part with a tendency towards the left side on the bottom part and towards the right side on the top part; while in February, March and April aggregation clusters began to regroup from the month of February, having infestation sites on the central part of the plot with a trend towards the bottom part, the next two months the aggregation clusters were distributed almost uniformly on the plot, there were some spots where a few aggregation clusters were present. Lastly, in May, aggregation clusters were located on the central part of the plot (Figure 2).

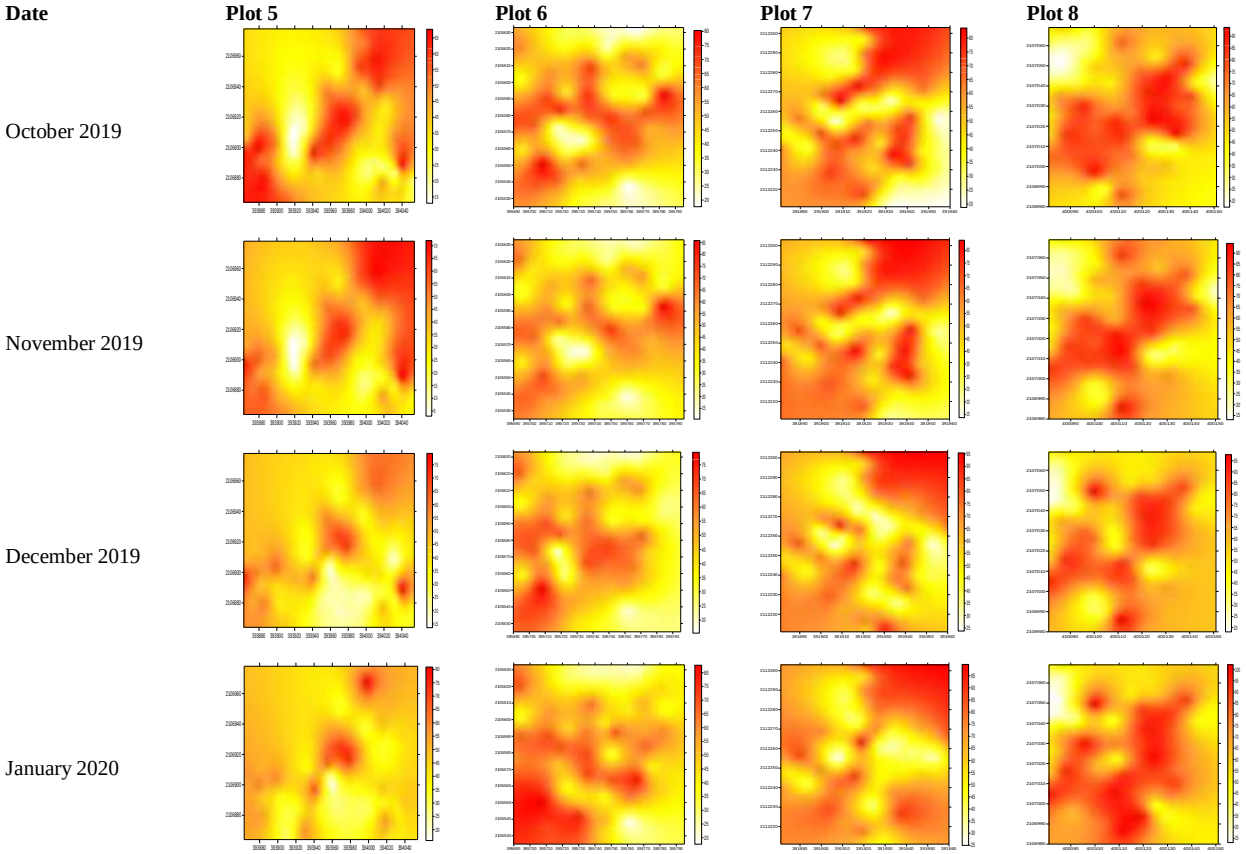

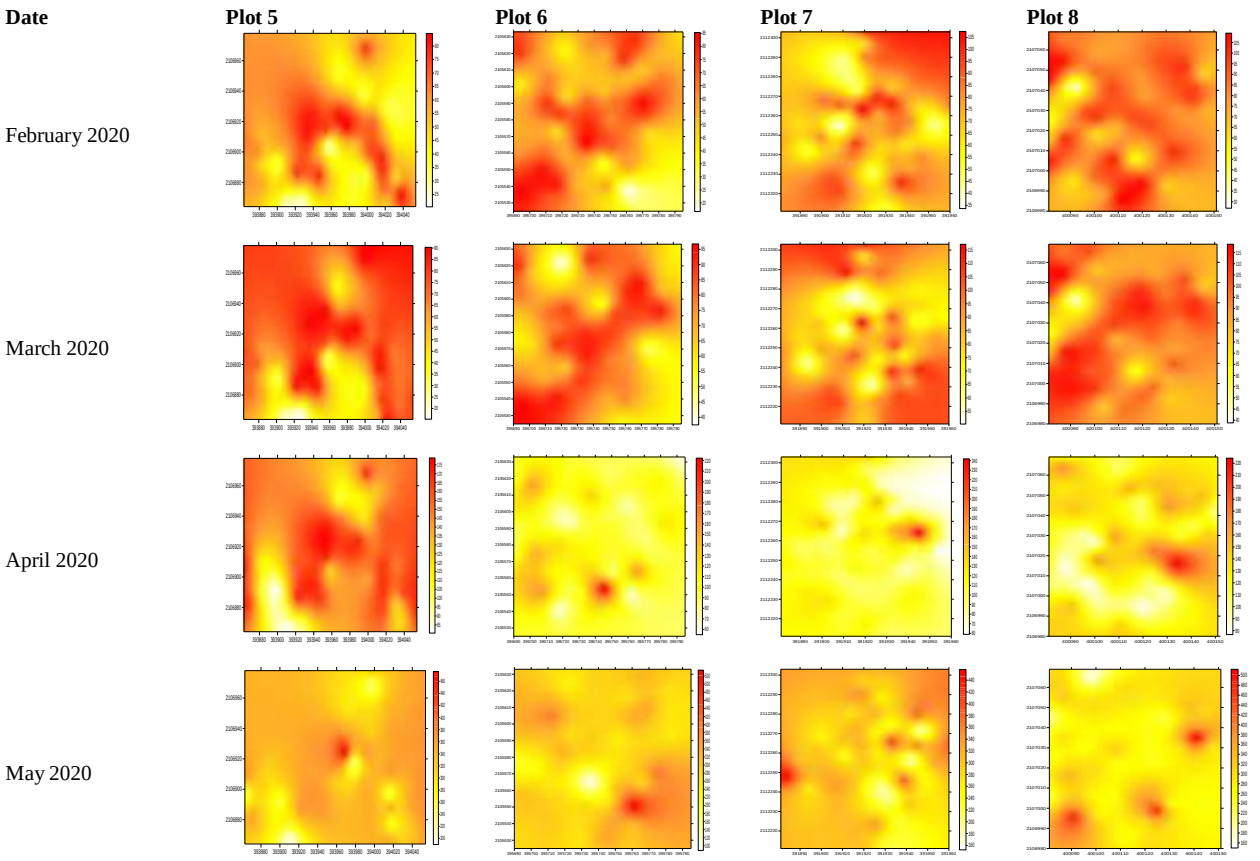

Figure 2. Density maps of *Oligonychus punicae* Hirst, in avocado crop, by sampling date in plots of Temascaltepec municipality.

Aggregation clusters were not distributed uniformly on the plot, presenting surface that was not infested, with which the planning of actions aimed at control and combat of *O. punicae* can be carried out. In Tenancingo municipality plot two presented the highest infestation in April with 98%, the plot with the lowest infestation was four in November with 83%. In Temascaltepec municipality the highest infestation percentage was on plot eight in March with 97% and the lowest percentage was in January with 78%, as it is observed on (Table 1.)

In the special analysis by distance indices (SADIE) the highest *Ia* observed in Tenancingo municipality was registered on plot three in May 1,70, the lowest on plot two in November 1,28; on the other side the highest *Ja* value was registered on plot four in April 1,24 and the lowest 1,05 on plot one in October.

In Temascaltepec municipality the highest *Ia* was registered on plot eight in November 1,72 and the lowest on plot five in May 1,30; similarly the highest *Ja* value was registered on plot five in April 1,24 and the lowest one in January on the same plot 1,06 (Table 3).

Table 3. Value of the *Ia* and *Ja* Indices and their Respective *Pa* and *Qa* Probabilities in the Red Spider mite Population (*Oligonychus punicae* Hirst), in Tenancingo Municipality (Plots 1, 2, 3, and 4) and Temascaltepec Municipality (Plots 5, 6, 7, and 8).

Plot	Date	I_a	P_a	J_a	Q_a
1	October 2019	1.34	0.005s	1.05	0.133ns
	November 2019	1.47	0.010s	1.10	0.178ns
	December 2019	1.65	0.014s	1.19	0.165ns
	January 2020	1.50	0.007s	1.06	0.209ns
	February 2020	1.36	0.006s	1.14	0.226ns
	March 2020	1.51	0.012s	1.15	0.249ns
	April 2020	1.29	0.011s	1.23	0.131ns
	May 2020	1.42	0.010s	1.20	0.262ns
2	October 2019	1.30	0.005s	1.10	0.275ns
	November 2019	1.28	0.014s	1.11	0.135ns
	December 2019	1.69	0.017s	1.09	0.280ns
	January 2020	1.36	0.009s	1.18	0.169ns
	February 2020	1.59	0.014s	1.17	0.238ns
	March 2020	1.33	0.011s	1.20	0.203ns
	April 2020	1.40	0.013s	1.08	0.153ns
	May 2020	1.29	0.010s	1.16	0.266ns
3	October 2019	1.56	0.016s	1.15	0.222ns
	Noember 2019	1.63	0.007s	1.23	0.241ns
	December 2019	1.48	0.015s	1.12	0.138ns
	Jannuary 2020	1.32	0.011s	1.11	0.271ns
	February 2020	1.49	0.018s	1.13	0.284ns
	March 2020	1.67	0.008s	1.10	0.257ns
	April 2020	1.38	0.013s	1.09	0.156ns
	May 2020	1.70	0.015s	1.20	0.246ns
4	October 2019	1.30	0.011s	1.21	0.142ns
	November 2019	1.55	0.005s	1.14	0.218ns
	December 2019	1.43	0.019s	1.13	0.204ns
	January 2020	1.64	0.008s	1.22	0.233ns
	February 2020	1.52	0.010s	1.19	0.188ns
	March 2020	1.41	0.013s	1.16	0.213ns
	April 2020	1.59	0.009s	1.24	0.147ns
	May 2020	1,60	0.012s	1.18	0.159ns
5	October 2019	1.32	0.011s	1.09	0.158ns
	November 2019	1.43	0.18s	1.13	0.134ns
	December 2019	1.62	0.010s	1.17	0.175ns
	January 2020	1.53	0.013s	1.06	0.167ns
	February 2020	1.49	0.014s	1.12	0.142ns
	March 2020	1.66	0.012s	1.08	0.208ns
	April 2020	1.57	0.007s	1.24	0.149ns
	May 2020	1.30	0.013s	1.19	0.229ns
6	October 2019	1.44	0.017s	1.15	0.289ns
	November 2019	1.69	0.015s	1.11	0.191ns
	December 2019	1,47	0.007s	1.22	0.242ns
	January 2020	1.45	0.012s	1.20	0.139ns
	February 2020	1.64	0.018s	1.16	0.251ns
	March 2020	1.34	0.011s	1.08	0.235ns
	April 2020	1.71	0.010s	1.14	0.132ns
	May 2020	1.50	0.015s	1.18	0.263ns
7	October 2019	1.65	0.010s	1.12	0.153ns
	November 2019	1.39	0.014s	1.11	0.180ns
	December 2019	1.51	0.016s	1.14	0.144ns
	January 2020	1.54	0.008s	1.09	0.196ns
	February 2020	1.46	0.008s	1.07	0.164ns
	March 2020	1.70	0.013s	1.23	0.214ns
	April 2020	1.65	0.011s	1.16	0.135ns
	May 2020	1.48	0.010s	1.20	0.237ns
8	October 2019	1.68	0.017s	1.18	0.172ns
	November 2019	1.72	0.019s	1.10	0.156ns
	December 2019	1.59	0.014s	1.13	0.257ns
	January 2020	1.41	0.009s	1.21	0.130ns
	February 2020	1.61	0.013s	1.11	0.249ns
	March 2020	1.37	0.006s	1.10	0.226ns
	April 2020	1.52	0.009s	1.15	0.143ns
	May 2020	1.40	0.016s	1.19	0.182ns

ns: non significant at 5%, s: significant at 5%.

Ia and *Ja* indices were significantly superior to one in all samples, which indicates spatial distribution of *O. punicae* populations presented aggregative patterns (*Ia* index) at various clustering aggregates (*Ja* index).

The aggregative pattern in the red mite spider population is shown on each map obtained (Fig, 1 and 2), which corroborates what is established by *Ia* and *Ja* indices, because the obtained maps show the different clustering aggregates in the population on the sampled months.

Discussion

The spatial pattern reflects the characteristic ecological property of a species therefore it is important to identify the space time dynamics of a pest in order to have a better understanding of spatial patterns of populations [21].

From the ecological point of view living beings are organized and made up of individuals of the same species in a given area, existing an exchange of genetic information between them, in the case of *O. punicae*, it can be found year round, with a highest incidence in dry and hot months of the year [4], regarding the sampled municipalities, such conditions are given in April and May when the number of mites is high, the months when this number is the lowest are October, November and December, because in these months temperatures are low; this was also observed by [23, 24].

The determination of the aggregated pattern in the spatial distribution model was carried out by means of the geostatistics. Compared with the estimation of the spatial distribution carried out with classical statistics, geostatistical methods provide a more direct measure of spatial dependence, because they take into account the bidimensional nature of the organisms through their exact spatial location and its independent of the relationship between mean and variance [7, 25].

With geoestatistics it is possible to describe the spatial continuity of any natural phenomeno, getting to know the way in which any continuous variable in space varies (spatial pattern) in one or several selected scales, with a level of detail that allows to quantify the spatial variance of the variable in different directions of space. Geostatistics uses functions to model this spatial variation, this functions are used to interpolate in space the variable value in non-sampling sites [26], in addition, it makes it possible to draw up useful maps of the spatial distribution of an organism [8].

Numerous investigations have been carried out in which they have worked the modelling of spatial distribution with insects, diseases and mites. In relation to insects, [27] carried out a study using geostatistics techniques to study spatial distribution of *Trips* spp. (Thysanoptera) and assessment of its control by predator *Amblyseius swirskii* in avocado crop; in diseases [28] worked with spatial distribution of the potential risk of wilting of avocado caused by *Phytophtora cinnamomi*; in mites, [29] carried out his work with the spatial distribution and population fluctuation of *Phyllocoptruta oleivora* (ashmead) (acari:eriophyidae) in citrics, [30] also worked with spatial distribution and effect of population densities of mite (*Tetranychus urticae* Koch) on feed corn yield. The use of techniques to model spatial distribution has proven to be an efficient tool to determine the spatial distribution of pests and diseases allowing to locate aggregation clusters in specific points with which management strategies can be carried out in economically important crops [25].

Spatial behavior under conditions of infestation of *O. punicae* in avocado presented an aggregated pattern, found on the top of the leaves, mostly ripe ones, the above allows to suggest that the handling of this mite can be achieved by directing its control to specific points or infestation sites where aggregation clusters are located, avoiding the widespread application of chemical products in avocado

commercial plots, helping minimize environmental deterioration and savings in inputs by producers, this agreed with [31], who worked with green mosquitoes (*Jacobiasca lubica*) on vine, where they indicated that knowing the infested surface on the maps is possible to establish the expenses and economic savings with respect to the application of insecticides, carrying out control measures directed at actually infested areas.

The values found in the nugget effect for the fitted semivariograms were equal to cero, which allows to consider that the sample error was minimal and the sample scale was appropriate, so it can be considered that the fitted models have a 98% reliability, consequently, it is valid to deduce that more than 90% of the total variance is due to the spatial dependence on the sampling scale used. In other words, over 90% of the variation in the distribution of the population of this mite was explained with the spatial structure established in the semivariograms [32-10, 25]. [14], in their work on the distribution of armyworm *Mythimna unipuncta* in corn, found nugget effect values close to cero, which points out that in its totality the variation of the pest distribution was explained by the spatial structure in the semivariograms. In addition to the foregoing, the geostatistical functions allow validating the experimental models that were obtained in the present paper Spherical and Gaussian in the different samplings [33-8, 25].

Dataset that fitted the Gaussian model, showed the spatial behavior in aggregation pattern, it is expressed continuously within the avocado plots, indicating a continuous progress of infestation of *O. punicae* in neighboring trees. This was also observed by [34], in their work on spatial modeling of Thrips, in husk tomato, where it was found that for most sampled dates, semivariograms fitted Gaussian model, noting that Thrips eggs are presented continuously within the plots with respect to the sampled points, inferring the existence of several factors that influenced the spread of females to oviposite more quickly; also [35] in his work about spatial stability and temporary distribution of thrips in avocado, points out that the samples that fitted the Gaussian model, reflect that the aggregation clusters are presented continuously within the plot.

Dataset that fitted the spherical model indicate that *O. punicae* aggregation occurs in greater quantity in certain areas of the plot with respect to the rest of the points considered in the sampling, that is, the aggregation clusters are random within the infestation site of the plot, these aggregation clusters show a rapid growth near the origin but as they move away they decrease as a result of the dissemination of the mite through the wind which results in infestation in specific sites, [36], in their work on armyworm (*Mythimna unipucta*) in corn, with respect to the spatial distribution of the dataset that fitted the spherical model, it points out that there are sites where armyworm manifests itself most. The above means that the aggregation clusters are random within the infestation site of the plot, possibly as a result of the type of dissemination that occurs through rapid growth close to the origin, resulting in infestations in specific areas. Marginal increases are decreasing, this is due to the temperature and phenology conditions of the crop. [27] in their work on spatial distribution of thrips and its control through the predator *Amblyseius swirskii* in avocado, in which assesses the effectiveness of the predator on the populations of thrips. They pointed out that the spherical model was the best fit for the dataset, indicating that aggregations of insects occur in certain areas of the plot with respect to the other points. The models that best fitted the datasets (Spherical and Gaussian), are indicative that *O. punicae* does not have an established spatial behavior, because climatic factors such as: temperature, humidity, exposure to sun, among other factors, influence the spatial distribution of the mite, therefore the present study is of great interest because it allows us to know patterns of movement and permanence at specific points with which preventive management programs can be performed, at the aggregation clusters and thereby maintain low infestation levels with economic savings.

The spatial dependence that *O. punicae* has is high because the result of the division of the value of the nugget effect by the value of the hill was less than 25% for all semivariograms. The values of the

nugget effect indicate that there is a high spatial dependency, which suggests that the populations of *O. punmicae* depend on each other and their aggregation level is high [33].

In the density maps obtained with the Kriging technique, the aggregation clusters of the population of *O. punicae* can be seen, with them we can visualize free areas and with presence of mites, with which we can deduct that *O. punicae* does not invade 100% of sampled plots. This was also appreciated by [6], who modelled the spatial distribution of the egg, nymph and adult stages of *Bactericera cockerelli* in potato, using geostatistical tools that allowed to visualize its spatial distribution through maps by means of kriging with which it was observed that the insect does not invade 100% of the surface of the plot, allowing to identify infested areas as well as infestation free areas. On the other hand, [25] indicate that the maps generated by sampling for the spatial modelling of thrips in avocado crop, allowed them to identify areas of infestation, finding that thrips is distributed in 100% of the plot. Similar results were found by [37], who investigated geospatial distribution and population density of *Thrips tabaci* in onion production using geostatistics. They found that the insect is present throughout the study plot, although at non-significant levels (population less than ten individuals per plant) where no insecticide application is required because of the very low population levels, concluding that there are areas where control should be applied in a targeted way based on the population density sampled.

The values obtained from the SADIE indices, *Ia* index was significantly greater than one in the different sampling, these results suggest that *O. punicae* is distributed in aggregative patterns. Regarding *Ja* index, similar results were obtained, it was significantly greater than one, which indicates that *O. punicae* spatial distribution is located on the entire surface concentrated at different aggregation clusters. The aforementioned is reflected on the obtained maps corroborating the points made by the indices *Ia* and *Ja* (Figures 1 and 2). Temporal stability of spatial distribution with SADIE has been reported in other papers such as [38], in which they wwith aggregation and temporal stability of the distribution of carabido beetles in field habitats; [14], with the spatial distribution and mapping of armyworm *Mythimna unipuncta* in corn and [35]BHO in the distribution of thrips in avocado crop.

Conclusions

Spatial distribution of *O. puncae* in avocado crop was determined with theoretical semivariograms, in which spatial behavior can be interpreted that the spatial behavior of the mite is found in aggregates in the plots, this was as well corroborated with the SADIE indices, because in these *O. punicae* presents a spatial pattern in aggregates with the populations distributed in several aggregation clusters, this can be visualized in the density maps generated through kriging.

Maps can be used to generate management programs, because they are a useful tool to aim control measures to specific areas, optimizing economical resources and reducing environmental impact of the use of agrochemicals, it also allows preventive actions which can result in low infestation levels. Finally if a balance is made of the economic savings and the impact on the environment, we could say that this type of work is important because traditional agriculture does not take into account time space variables.

Acknowledgments

The financial support of the Science and Technology National Council (CONACYT) for the scholarship granted for the realization of doctoral studies is gratefully acknowledged, to the Faculty of Agricultural Sciences of the Autonomous University of the State of Mexico (UAEMex) as well as the Avocado producers of the Tenancingo and Temascaltepec municipalities, for all the facilities provided.

Literature Cited

1. SIAP (2017). Statical yearbook of agriculture production (Avocado). http://infosiap.siap.gob.mx/aagricola_siap_gb/icultivo/index.jsp.
2. Equihua, MA, Estrada, VE, Chaires, GM., Acuña Soto, JA. (2016). behavior of *Araptus schwartzi* blackman (coleoptera: curculionidae: scolytinae) in avocado seeds (Hass) In different stages of maturity. *Folia Entomológiaca Mexican (new serie, 2(2)*, 33-38.
3. Cerna, E, Badii, M, Ochoa, Y, Aguirre, L, Landeros, U. (2009). table of the life, *Oligonycchus punicae* Hirst (Acari: Tetranychide) in avocado leaves (Persea American mill) Hass variety, strong and creole. University and science *25*, 133-140.
4. Valdivia Bouriga E, Sandoval Vargas M, Ortega Ayala JJ, Chávez Lara BN., Gutiérrez Contreras M, (2016). Evaluación De Insecticidas Orgánicos Para El Control De Ácaros En El Cultivo Del Aguacate. Entomología mexicana, 3, 125-130.
5. GONZÁLEZ, OE. (2012). Geostastical study of the spatial distribution of adult red spider. (Oligonychus Punicae Hirst) demage on the avocado crop (Persea American Mill) in the east zone of the state of Michoacán, Mexico. (professional thesis). Faculty of Agricultural Sciences, Autonomous University State of Mexico, 117.
6. Ramírez Davila, JF., Figueroa, DK. (2013). (2013) Modeling is the distribution special of Bactericera cockerelli Sulc (Hemiptera:Triozidae) in potato in the State of Mexico. Agricultural Center, *40(3)*, 57-70.
7. Ramirez Davila, JF, Solares Alonso, VM, Figueroa Figueroa, DK., Sánchez Pale, JR. (2013). Spatial behavior of thrips (Insecta: Thysanoptera) in commercial avocado plantations (Persea americana Mill.) In: Zitacuaro, Michoacán, Mexico. Acta zoologica Mexicana, 29(3), 545-562.
8. Ramirez Davila, JF, Porcayo, E., Sánchez, JR. (2013). Modeling is the distribution special of *Bactericera cockerelli* Sulc. (Hemiptera: Triozidae) *en Solanum tuberosum* L. (Solanales: Solanaceae). Revista de la Facultad de Agronomía, *45*,13-27.
9. Maldonado, FI, Ramírez, Davila, JF, Rubí, M; Xanat, N., Lara, V. (2016). Spatial distribution of trips in avocado in Coatepec Harinas State of Mexico, Mexican magazine of Agricultural Sciences *7*,845-856.
10. Liebhold, A, Sharov, A (1998). *Testing for correlation in the presence of spatial autocorrelation in insect count data. in: Population and community Ecology for insect management and conservation (J. Baumgartner, P. Brandmayr y B. F. J. Manly eds.)* Inglaterra: Balkema, Rotterdam.
11. Isaaks, E., Srivastava, M. (1989). *An introduction to applied geostatistics.* Estados Unidos: Oxford Univ. Press.
12. Journel, AG., Huijbregts, CJ. (1978). *Mining geostatistics. Academic Press.* London, Reino Unido, 600.
13. ENGLUD, E.; SPARKS, A. 1988. GEO-EAS (Geostatistical Environmental Assessment Software) User´s Guide. U.S. Environmental Protection Agency document EPA/600/4-88/033. Environmental Monitoring Systems Laboratory, Las Vegas, NV. p. 130.
14. Esquivel, HV, Jasso, GY. (2014). Spatial distribution and mapping of soldierworm in six localities of the State of Mexico, in 2011. Mexican Journal of Agricultural Sciences, *5(6)*, 923-935.
15. Hevesi, JA, Istok, JD., Flint, AL. (1992). Precipitation estimation in mountainous terrain using multivariate geostatistics. Part. I. Structural analysis. *Journal of Applied Meteorology, 31(7)*, 661-676. https://doi.org/10.1175/1520-0450(1992)031<0661:PEIMTU>2.0.CO;2
16. Samper, F, Carrera, J. (1990). geostastitical applications the underground hydrology. Spain: CIMNE
17. Lopez, GF, Jurado, EM, Atenciano, S, García, FA, Sánchez, MS., García LT. (2002). Spatial variability of agricultural soil parameters in southern Spain. *Plant and Soil,*

246(1), 97-105.
18. López SF, Jurado, EM, Atenciano, S, García, FA, Sánchez, M, García, TL, (2002). Spatial variability of agricultural soil parameters in southern Spain. *Plant and Soil. 246,* 97-105.
19. Sánchez, P, Ramírez Davila, JF, González, A., De León, C. (2011). Spatial distribution of head smut (*Sporisorium reilianum*) of corn in Mexico. *International journal of Agriculture and Natural Resources. 38(2),* 5-14.
20. Perry, J, Bell, E, Smith, R, Woiwod, I, (1996). SADIE Software to measure and model spatial pattern. *Asp Appl Biol. 46,* 95-102.
21. Perry, J. 1998. Measures of Spatial Pattern for Counts. *Ecology.79(3),* 1008-1017.
22. Morlans, M.C. (2004). Introduction of population ecology University University edition national university of catamarca science.
23. Reyes, J, Rubí, M., Salgado, M. (1993). *Dynamic population of spider mites (Oligonychus punicae Hirst) in 16 avocado selections. Foundation* Salvador Sánchez Colín CICTAMEX, S.C.
24. CORIA, A, AYALA, A. (2010). *Management of avocado in Mexico SAGARPA*. Uruapan Michoacán, México. Technical Brochure
25. Rivera, MR, Ramírez Dávila, JF, Rubí, AM, Dominguez, LA, Acosta Guadarrama, A. D., Figueroa-Figueroa, D K. (2017). Spatial modeling of trips, (Insecta:Thysanompera) in avocado cultivation, (*Persea americana*). Revista Colombiana de Entomología. *43(2),*131-140.
26. Gallardo, A. (2006). Geoestatitical ecosystems *15(3),* 48-58.
27. Acosta Guadarrama, AD, Ramírez Dávila, JF, Rivera, MR, Figueroa Figueroa, DK, Lara, DV, Maldonado Zamora, FI, et al.2017. Spatial distribution of trips spp, (Thysanoptera) and evaluation of the control by the predator, *Amblyseius swirskii* in the cultivation of avocado in Mexico. *42(2),* 435-446.
28. Osorio Almaza, NL, Burbano, FO, Arcilla, AM, Vázquez, AM, Carrascal, PF., Romero, J. (2017). spatial distribution of potential risk of an avocado withering caused by *Phytophthora cinnamomi* In the sub-region of Montes de Maria, Colombian magazine. Revista Colombiana de Ciencias Hortícolas. *11(2),* 273-285.
29. Landeros, J, Balderas, J, Mohammad, HB, Sánchez, VM, Guerrero, E, Flores, AE, (2003). Spatial distribution and population fluctuation of in citrus of *Phyllocoptruta oleivora* (ashmead) (acari: eriophyidae) in citrus of güemez, Tamaulipas. *Zoological Mexican Act. 89,* 129-138.
30. López López, OV, Cerna CE, Flores CR, Gevara Acevedo, LP., Landeros, FJ. (2011). Spatial and distribution density effects of population in performance of fodder corn. *Tetranychus urticae* agriaria magazine *8(1),* 18-23.
31. Ramírez, JF, Porcayo, E. (2009). spatial behavior of green mosquito larvae Jacobiasca lybica, in an drying vineyard in Andalucía Spain. Science *ergo sum. 16 (2),* 164-170.
32. Oliver, M, Webster, R. (1991). How geostatistics can help you. *Soil Use Manag. 7,* 206-217.
33. Rossi, RE, Mulla, DJ, Journel, AG., Franz, EH. (1992). Geostatical tools for modeling and interpreting ecological spatial dependence. *Ecological Monographs, 62(2),* 277-314.
34. JIMÉNEZ, R, RAMÍREZ, J, SÁNCHEZ, J, SALGADO, M., LAGUNA, A. (2013). Spatial modeling of Frankliniella occidentalis (Thysanoptera: Thripidae) on husk tomato using geostatistical techniques. Revista Colombiana de Entomología *46*, 29-44.
35. MALDONADO Z., RAMÍREZ, J.F, LARA, AV, RIVERA, R.; ACOSTA, AD, FIGUEROA, DK, RUBÍ, M y TAPIA, A. (2017). Spatial stability and temporary distribution of trips 1 and the avocado cultivation in the state of Mexico. Southwestern Entomologistl. 42 (2), 446-462.
36. RAMÍREZ, JF., ESQUIVEL, V. (2012). Spatial modeling of army worm, (*Mythimna unipuncta*) in the cultivation of corn in the three municipalities of the State of Mexico, Boletín del Museo de Entomología de la Universidad del Valle in 2008. *13 (1*) 1-15.
37. PAZ, R, ARRIECHE, N. (2017). Spatial distribution of *Thrips tabaci* (Lindeman) 1888 (thysanoptera: thripidae) in Quibor in Lara state, Venezuela. *Bioagro 29,* 123-128.

38. THOMAS, CF, PARKINSON, L, GRIFFITHS, J, FERNANDEZ, A., MARSHALL, J. (2001). Aggregation and temporal stability of carabid beetle distributions in field and hedgerow hábitats. *38*, 100-116.
39. PERRY, J. (1995). Analysis by distance indices. *J Anim Ecol, 64 (3),* 303-314.
40. QUERO, L. (2006). SADIE as a tool for quantity spatial heterogeneity: case studies in the Sierra Nevada national park (Granada, España). Ecosystems, *15*, 40-47.